

# Quasi Periodic Oscillations in Low Mass X-Ray Binaries and Constraints on the Equation of State of Neutron Star Matter

Christoph Schaab and Manfred K. Weigel

*Institut für theoretische Physik, Ludwig-Maximilians Universität München, Theresienstr. 37, D-80333 München, Germany*  
*email: schaab@gsm.sue.physik.uni-muenchen.de*

7 October 2018

## ABSTRACT

Recently discovered quasi periodic oscillations in the X-ray brightness of low mass X-ray binaries are used to derive constraints on the mass of the neutron star component and the equation of state of neutron star matter. The observations are compared with models of rapidly rotating neutron stars which are calculated by means of an exact numerical method in full relativity. For the equations of state we select a broad collection of models representing different assumptions about the many-body structure and the complexity of the composition of super dense matter. The mass constraints differ from their values in the approximate treatment by  $\sim 10\%$ . Under the assumption that the maximum frequency of the quasi periodic oscillations originates from the innermost stable orbit the mass of the neutron star is in the range:  $M \sim 1.92 - 2.25 M_{\odot}$ . Especially the quasi periodic oscillation in the Atoll-source 4U 1820-30 is only consistent with equations of state which are rather stiff at high densities which is explainable, so far, only with pure nucleonic/leptonic composition. This interpretation contradicts the hypothesis that the protoneutron star formed in SN 1987A collapsed to a black hole, since this would demand a maximum neutron star mass below  $1.6 M_{\odot}$ . The recently suggested identification of quasi periodic oscillations with frequencies around 10 Hz with the Lense-Thirring precession of the accretion disk is found to be inconsistent with the models studied in this work, unless it is assumed that the first overtone of the precession is observed.

**Key words:** stars: neutron – equation of state – gravitation – stars: rotation – accretion, accretion discs – X-ray: stars

## 1 INTRODUCTION

Neutron stars contain matter in one of the densest forms found in the universe. Their central density ranges from a few times the density of normal nuclear matter to about one order of magnitude higher, depending on the star's mass and the equation of state (EOS). Neutron stars therefore provide us with a powerful tool for exploring the properties of such dense matter. In the last decades, this tool was applied to, among other topics, the determination of the EOS of dense, charge neutral,  $\beta$ -equilibrated matter by means of comparing the theoretical predicted properties with observations of neutron stars. This was attempted by studying, for example, the maximum stable star mass (van Kerkwijk et al., 1995), the minimum rotation period (Friedman et al., 1986; Weber & Glendenning, 1992), or the thermal behaviour (Tsuruta 1966, Schaab et al. 1996, Page 1997; see Balberg, Lichtenstein & Cook 1998 for a recent review).

Recently, Strohmayer et al. (1996) and Van der Klis et

al. (1996) discovered with the Rossi X-ray Timing Explorer (RXTE) kilohertz quasi-periodic oscillations (QPOs) in the X-ray brightness of low-mass X-ray binaries (LMXBs, see van der Klis 1997 for a recent review). In subsequent observations, three QPOs were often detected simultaneously in a given source. The frequency separation between both QPOs is almost constant, although the frequencies of the two QPOs themselves vary by several hundred Hertz. Up to now, the only exceptions are the Atoll sources 4U 1608-52 and 4U 1735-44 and the Z-source Scorpius X-1 in which the frequency separation varies with the luminosity by roughly  $\pm 15\%$  (Méndez et al., 1998c; van der Klis & Wijnands, 1997; Ford et al., 1998b). Psaltis et al. (1998) found that the QPO data of the other LMXBs are consistent both with being constant and with varying by a similar fraction as in the two sources quoted before. The frequency of oscillations during type I X-ray bursts detected in some sources are consistent with the frequency separation of the two QPOs or with

its first overtone. Only in the source 4U 1636-536 the averaged frequency separation,  $\Delta\nu = 251$  Hz, and the half of the frequency in type I bursts,  $\nu_{\text{burst}} = 581$  Hz, differ by approximately 15% (Méndez & van Paradijs, 1998). In the power spectrum of bursts of the same source Miller (1998) found a second signal at 290 Hz  $\sim 1/2\nu_{\text{burst}}$ . These observations strongly favour the beat frequency model where the frequency separation between the two QPOs originates from the stellar spin, whereas the higher QPO is produced by accreting gas in a stable, nearly circular orbit around the neutron star. Though, it has to be clarified how the slightly varying frequency separation and the small deviation of the frequency separation from the burst frequency can be incorporated into this model.

Beside the two kilohertz QPOs and the burst oscillations, also QPOs with frequencies of a few tens of Hertz were detected in some sources. Their frequencies correlate with the high frequency kilohertz QPOs. These low frequency QPOs were interpreted by Stella & Vietri (1998) to originate from the Lense-Thirring precession of the accreting disc due to the frame dragging effect of the rapidly spinning neutron star (Lense & Thirring, 1918).

Both, the identification of the high frequency kilohertz QPOs with the orbital frequency of a stable circular orbit and the low frequency QPOs with the frame dragging frequency of the same orbit allow to constrain the mass of the neutron star and also the EOS of neutron star matter (Lamb et al., 1998; Stella & Vietri, 1998). If the evidence for the detection of QPOs of the innermost stable circular orbit in the sources 4U 1608-52, 4U 1636-536 (Kaaret et al., 1997), and 4U 1820-30 (Zhang et al., 1998b) can be confirmed by future observations, the constraints are rather severe, allowing only a few stiff EOSs.

The frequency separation of the two kilohertz QPOs show that the neutron star in LMXBs are rapidly rotating with periods ranging from 2.5 ms to 4 ms. It can therefore be expected that the geometry of the neutron star and its exterior space time is non-spherical. Since the innermost stable orbit is located at only a few kilometres above the star's surface, the deviation from the Kerr space time are large and should not be neglected. In order to compare theoretical neutron star models with QPO observations, a completely general relativistic calculation of the rotating neutron star structure and space time geometry is therefore necessary.

In order to study the impact and the discrimination power of the QPO data in greater detail, we select a broad collection of modern EOSs, which were obtained utilising numerous assumptions about the dynamics and composition of super dense matter. To mention several, these are: the many-body technique used to determine the EOS; the model for the nucleon-nucleon interaction; description of electrically charge neutral neutron star matter in terms of either only neutrons and protons in generalised chemical equilibrium ( $\beta$  equilibrium) with electrons and muons, or nucleons, hyperons and more massive baryon states in  $\beta$  equilibrium with leptons; hyperon coupling strengths in matter; inclusion of meson ( $\pi$ ,  $K$ ) condensation; treatment of the transition of confined hadronic matter into quark matter; and assumptions about the true ground state of strongly interacting matter (i.e., absolute stability of strange quark matter relative to baryon matter).

The paper is organised as follows. In Sect. 2 we sum-

marise the equations which govern the space time structure and compare the approximate values of the orbital frequencies, the radius of the innermost stable orbit, and the Lense-Thirring precession frequencies with the respective values from the exact numerical solution of Einstein's equations. The physics of the EOSs is discussed in Sect. 3. The high frequency kilohertz QPOs and their interpretation in combination with their compatibility with the different EOSs are discussed in Sect. 4. The implications of the identification of the low frequency QPOs with Lense-Thirring precession are presented in Sect. 5. We summarise our results, the constraints to the neutron star masses, and the conclusions concerning the neutron star EOS in Sect. 6.

## 2 SPACE TIME AROUND RAPIDLY ROTATING NEUTRON STARS

### 2.1 Einstein Equations

The stationary, axis-symmetric, and asymptotic flat metric in quasi isotropic coordinates reads

$$ds^2 = -e^{2\nu} dt^2 + e^{2\phi} (d\varphi - N^\varphi dt)^2 + e^{2\omega} (dr^2 + r^2 d\theta^2), \quad (1)$$

where the metric coefficients  $g_{\mu\nu} = g_{\mu\nu}(r, \theta)$  are functions of  $r$  and  $\theta$  only. The metric coefficients are determined by the Einstein equation ( $c = G = 1$ )

$$\mathbf{G} = 8\pi\mathbf{T}, \quad (2)$$

and the energy-momentum conservation

$$\nabla \cdot \mathbf{T} = 0, \quad (3)$$

where  $\mathbf{T} = (e + p)\mathbf{u} \otimes \mathbf{u} + p\mathbf{g}$  is the stress-energy tensor of an ideal fluid with the 4-velocity

$$\mathbf{u} = \Gamma e^{-\nu} \mathbf{e}_t + \Omega \Gamma e^{-\nu} \mathbf{e}_\varphi, \quad (4)$$

the energy density  $e$ , and the pressure  $p$ . The Lorentz factor  $\Gamma$  is given by  $\mathbf{u} \cdot \mathbf{u} = -1$ , hence

$$\Gamma = \left(1 - e^{2(\phi-\nu)} (\Omega - N^\varphi)^2\right)^{-\frac{1}{2}}. \quad (5)$$

$\Omega = u^\varphi/u^t$  is the angular velocity of the fluid with respect to an observer at infinity. The proper velocity  $U$  of the fluid with respect to the local Eulerian Observer  $\mathfrak{D}_o$  (Smarr & York, 1978) is given by the equation

$$U = \frac{1}{g_{\varphi\varphi}^{1/2} \Gamma} \mathbf{e}_\varphi \cdot \mathbf{u} = e^{\phi-\nu} (\Omega - N^\varphi). \quad (6)$$

Note that if the fluid were at rest with respect to the Observer  $\mathfrak{D}_o$ ,  $U = 0$ , it would not necessarily be at rest for an inertial observer at infinity, since  $\Omega = N^\varphi \neq 0$ . This phenomena of *dragging of the inertial frame* was first studied by Lense & Thirring (1918) and turns out to be important for the investigation of the Lense-Thirring precession of the accreting disc (see Sect. 5).

The four non-trivial Einstein equations together with the energy-momentum conservation are solved via a finite difference scheme (Schaab, 1999). We follow Bonazzola et al. (1993) in compactifying the outer space to a finite region by using the transformation  $r \rightarrow 1/r$ . The boundary condition of approximate flatness can then be exactly fulfilled.

The neutron star model is uniquely determined by fixing one of the parameters: central density, gravitational mass, baryon number, Kepler orbiting frequency at the star's equator or at the marginally stable radius, as well as one of the parameters: angular velocity, angular momentum, or stability parameter  $t = T/|W|$ . The models of maximum mass and/or maximum rotation velocity can also be calculated.

## 2.2 Stable Circular Orbits

Since  $\mathbf{e}_t$  and  $\mathbf{e}_\varphi$  are Killing vectors, the components  $p_t$  and  $p_\varphi$  of the 4-momentum of a freely falling particle are constants of motion and can be identified with the negative of the specific energy  $E$  (in units of the rest mass  $m_0$ ) and the specific angular momentum  $L$ , respectively. For a particle motion confined to the equatorial plane the geodesic equation  $p_\mu^\mu = -1$  yields:

$$e^{-2\omega} p_r^2 = -1 + e^{-2\nu} (E - N^\varphi L)^2 - e^{-2\phi} L^2 = e^{-2\nu} V(E, L, r), \quad (7)$$

where  $V$  is the effective potential for the particle motion (Misner et al., 1973, pp. 655). A circular orbit,  $p_r = 0$ , is given by the expression (4) for the 4-velocity of the fluid inside the star. Then, the specific energy  $E$  and angular momentum  $L$  can be expressed in terms of the Lorentz factor  $\Gamma$  (Eq. 5) and the proper velocity  $U$  (Eq. 6):

$$E = \Gamma (e^\nu + e^\phi N^\varphi U) \quad (8)$$

$$L = e^\phi \Gamma U. \quad (9)$$

The circular orbit exists if  $V_{,r} = 0$ , thus\*

$$-\phi_{,r} U^2 + e^{\phi-\nu} N_{,r}^\varphi U + \nu_{,r} = 0. \quad (10)$$

The proper velocity  $U$  of a particle corotating with the star is given by

$$U = \frac{e^{\phi-\nu} N_{,r}^\varphi + \sqrt{e^{2(\phi-\nu)} (N_{,r}^\varphi)^2 + 4\phi_{,r} \nu_{,r}}}{2\phi_{,r}}. \quad (11)$$

The circular orbit is stable, if  $V_{,rr} < 0$  with (see also Cook, Shapiro & Teukolsky 1992 and Datta, Thampan & Bombacci 1998)

$$V_{,rr} = 2e^{2\nu} \Gamma^2 (e^{\phi-\nu} U N_{,rr}^\varphi - e^{2(\phi-\nu)} U^2 (N_{,r}^\varphi)^2 + \nu_{,rr} + 2(\nu_{,r})^2 - U^2 \phi_{,rr} + 2U^2 (\phi_{,r})^2 - 4\nu_{,r} \phi_{,r} U^2). \quad (12)$$

The zero of  $V_{,rr}$  determines the radius  $r^{\text{ms}}$  of the innermost stable or marginally stable circular orbit. The Kepler frequency  $\nu_K$  of a circular orbit as measured by a distant observer is given by the proper velocity  $U$  through the expression

$$\nu_K = \frac{1}{2\pi} (e^{\nu-\phi} U + N^\varphi), \quad (13)$$

and the Lense-Thirring precession frequency by

$$\nu_{\text{LT}} = \frac{1}{2\pi} N^\varphi. \quad (14)$$

\* We use the usual convention, that  $\cdot_{,\mu}$  represents the partial differential  $\partial/\partial x^\mu$ .

The respective values at the innermost stable orbit with radius  $r^{\text{ms}}$  are denoted by  $\nu_K^{\text{ms}}$  and  $\nu_{\text{LT}}^{\text{ms}}$ , respectively. The circumferential radius  $r_{\text{circ}}$  of the object is linked to the equatorial coordinate radius  $r$  by the expression

$$r_{\text{circ}} = e^\phi r. \quad (15)$$

## 2.3 Approximate Expressions

Though we shall use the exact expressions for  $\nu_K$ ,  $\nu_{\text{LT}}$ ,  $\nu_K^{\text{ms}}$ , and  $\nu_{\text{LT}}^{\text{ms}}$  in our investigation, we give also, for the purpose of comparison, the approximate expressions valid to first order of the dimensionless angular momentum  $j = J/M^2$ , where  $J$  and  $M$  denotes the angular momentum and gravitational mass, respectively. The approximate expressions have the advantage to constrain the mass and the angular momentum independently of the EOS. To first order in  $j$  the corresponding expression are (Miller et al., 1998b):

$$\nu_K = \frac{1}{2\pi} \left( \frac{M}{r_{\text{circ}}^3} \right)^{\frac{1}{2}} \left( 1 - \left( \frac{M}{r_{\text{circ}}} \right)^{\frac{3}{2}} j \right), \quad (16)$$

$$\nu_{\text{LT}} = \frac{2}{2\pi} \frac{M^2}{r_{\text{circ}}^3} j, \quad (17)$$

$$r_{\text{circ}}^{\text{ms}} = 6M \left( 1 - \left( \frac{2}{3} \right)^{\frac{3}{2}} j \right), \quad (18)$$

$$\nu_K^{\text{ms}} = \frac{6^{-\frac{3}{2}}}{2\pi} \frac{1}{M} \left( 1 + 11 \times 6^{-\frac{3}{2}} j \right), \quad (19)$$

$$\nu_{\text{LT}}^{\text{ms}} = \frac{6^{-3}}{\pi} \frac{j}{M}. \quad (20)$$

## 3 EQUATIONS OF STATE

### 3.1 Neutron Star Matter

The EOS of neutron star matter is the basic input quantity to the structure equations discussed in Sect. 2. Its knowledge over a wide range of densities is necessary. Whereas the density at the star's surface corresponds to the density of iron, the density in the centre of a very massive star can reach 15 times the density of normal nuclear matter. Since neutron star matter in chemical equilibrium (i.e. generalized  $\beta$ -equilibrium) is highly isospin-asymmetric and may carry net-strangeness its properties cannot be explored in laboratory experiments. Therefore, one is left with models for the EOS which depend on theoretically motivated assumptions and/or speculations about the behaviour of super dense matter. One main source of uncertainty is the competition between non-relativistic versus relativistic models. Though both treatments give satisfactory results for normal nuclear densities, they provide quite different results if one extrapolates to higher densities (see, e.g. Huber et al. 1998). Moreover, one encounters strong differences in the high density regime depending on the underlying dynamics, the many-body approximation and the assumptions about the composition. The simplest approach describes neutron star matter by pure neutron matter. Since pure neutron matter is certainly not the true ground state of neutron star matter, it will quickly decay by means of the weak interaction into chemically equilibrated neutron star matter, whose fundamental constituents – besides neutrons – are protons,

hyperons and possibly more massive baryons. Even a transition to quark matter (so-called hybrid stars) and the occurrence of pion- or kaon-condensates is possible.

The cross section of a neutron star can be split roughly into three distinct regimes (Börner, 1973; Weber & Glendenning, 1993). The first one is the star’s outer crust, which consists of a lattice of atomic nuclei and a Fermi liquid of relativistic, degenerate electrons. The inner crust extends from neutron drip density,  $\rho = 4.3 \times 10^{11} \text{ g cm}^{-3}$ , to a transition density of about  $\rho_{\text{tr}} = 1.7 \times 10^{14} \text{ g cm}^{-3}$  (Pethick et al., 1995). Beyond this transition density  $\rho_{\text{tr}}$  one enters the star’s third regime, that is, its core where all atomic nuclei have dissolved into their constituents, protons and neutrons. Furthermore, as outlined just above, due to the high Fermi pressure the core will contain hyperons, eventually more massive baryon resonances, and possibly a gas of free up, down and strange quarks.

The EOS of the outer and inner crust has been studied in several investigations and is rather well known. We shall adopt for these regions the models derived by Haensel & Pichon (1994) and by Negele & Vautherin (1973), respectively. The models for the EOS of the star’s core are discussed in detail in Schaab et al. (1996).

An overview of the collection of EOSs used in this paper for the core region is given in Tab. 1. We have chosen a representative collection of different models in order to check which EOSs are compatible with the QPOs and their theoretical interpretation.

An important characteristic of relativistic models is the appearance of a new saturation mechanism. In relativistic theories the repulsive force is caused by the exchange of vector mesons coupled to the baryon densities, whereas the attraction is coupled to the scalar densities by means of the scalar mesons. Hence, the repulsion increases with increasing density with respect to the attraction. Since non-relativistic treatments do not distinguish both kinds of densities, one has to introduce adhoc forces depending explicitly on density in order to reproduce properties of saturated nuclear matter.

The potential parameters and coupling constants in the pure nucleonic sector are adjusted to nucleon–nucleon scattering data and properties of the deuteron in the case of the non-relativistic microscopic models and the relativistic Brückner-Hartree-Fock models. In this sense, these models are called *parameter free*. For the Hartree- and the Hartree-Fock approximation, as well as for the Thomas-Fermi model such an adjustment is not possible, since the free force parameters would not yield saturation of nuclear matter. In such more phenomenological approximations the coupling constants are adjusted to properties of saturated nuclear matter or atomic nuclei (Weber & Weigel, 1989; Schaffner & Mishustin, 1996; Myers & Swiatecki, 1996). In a more recent and more elaborate investigation (Huber et al., 1998), the adjustment was performed with respect to properties of neutron star matter at 2–3 times nuclear density known from relativistic Brückner-Hartree-Fock calculations. Relativistic Brückner-Hartree-Fock calculations cannot be performed over the whole density range at present, since an inclusion of hyperons leads to rather complex equation systems. Even for pure nucleonic matter, the self consistent method is numerically stable up to 2–3 times nuclear density only (Huber et al., 1998).

Since the coupling constants of hyperons are not obtain-

able from properties of normal nuclei and data of hypernuclei are relatively scarce, one has a greater freedom in the selection of parameter sets in the hyperonic sector. From a theoretical standpoint one may first utilise the SU(6) symmetry of the quark model for the vector coupling constants and adjust the  $\sigma$ -coupling from the binding energy of the  $\Lambda$  hyperon in nuclear matter. It turns out, however, that this procedure gives different  $\sigma$ -couplings depending on the chosen many-body approximation. Therefore, it seems reasonable to vary both couplings with the constraint of the  $\Lambda$  binding energy in nuclear matter in such phenomenological many-body theories. A further constraint in this procedure is the compatibility with the allowed neutron star masses (for more details, see Huber et al. 1998 and Huber 1998). The coupling constants for the strange mesons can be obtained to a certain extent from the data of double  $\Lambda$ -hypernuclei (Schaffner & Mishustin, 1996). Batty et al. (1994) claim some doubts on the existence of  $\Sigma$  hyperons in neutron star matter. However, the disappearance of  $\Sigma$  hyperons would only slightly change the EOS (Balberg & Gal, 1997). A further open question is still the existence of  $\Delta$  isobars in the interior of neutron stars. In relativistic Hartree treatments, the isospin unfavoured  $\Delta^-$  isobar does not appear because of the rather large  $\rho$ -coupling, which is necessary to reproduce the empirical symmetry coefficient (Huber et al., 1998).  $\Delta$  isobars are therefore often neglected a priori in relativistic Hartree treatments (Schaffner & Mishustin, 1996). However, in relativistic Hartree-Fock approximations, the  $\rho$ -coupling becomes smaller due to the exchange contributions. For that reason, the charge favoured  $\Delta^-$  may now enter the composition depending on the behaviour of the effective  $\Delta$ -mass in neutron star matter, which is quite uncertain (Huber et al., 1998).

The possibility of a transition of confined hadronic matter into quark matter at high densities is included in the EOS labelled  $G_{\text{B180}}^{\text{K240}}$  (Glendenning, 1995) (so-called hybrid stars). The transition was determined for a bag constant of  $B^{1/4} = 180 \text{ MeV}$  which places the energy per baryon of strange quark matter at 1100 MeV, well above the energy per nucleon in saturated nuclear matter as well as in the most stable nucleus,  $^{56}\text{Fe}$  ( $E/A \approx 930 \text{ MeV}$ ). This model predicts a transition to a mixed phase consisting of quark matter and hadronic matter at a density as low as  $1.6 n_0$ . The pure quark-matter phase is reached at a density of about  $10 n_0$ , which is close to the central density of the heaviest and thus most compact star constructed from such an EOS. A phase transition to pion condensation is accounted for in  $G_{300}^{\pi}$ . This EOS predicts a phase transition at  $n \approx 1.3 n_0$ . The possibility of absolutely stable strange quark matter will be considered in the following section.

The stiffness of the EOS depends strongly on the internal degrees of freedom. Generally, the more degrees of freedom are taken into account the softer the EOS becomes (s. Fig. 1). A softer EOS, in turn, leads to lower maximum neutron star masses and, for fixed mass, to higher central densities.

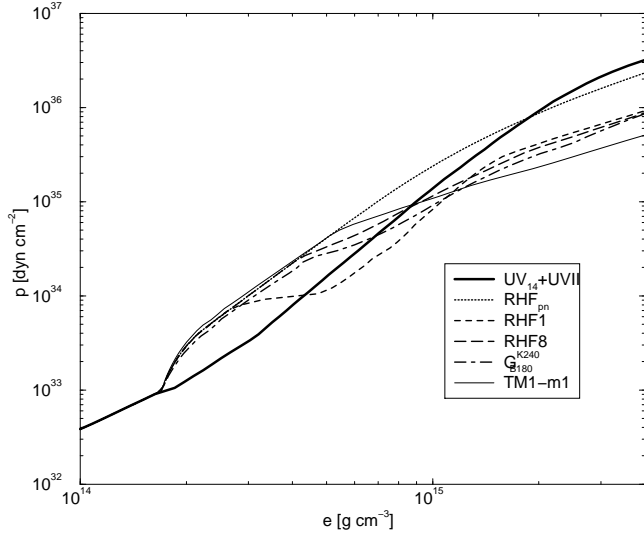
### 3.2 Strange Stars

The hypothesis that strange quark matter may be the absolute ground state of the strong interaction (not  $^{56}\text{Fe}$ ) has been raised independently by Bodmer (1971) and Witten

**Table 1.** Dynamics and approximation schemes for EOSs derived for the cores of neutron stars

EOS	Composition	Interaction	Many body approach	Reference
UV <sub>14</sub> +UVII	p, n, e <sup>-</sup> , μ <sup>-</sup>	Urbana V <sub>14</sub> and Urbana VII	NRV	Wiringa, Fiks & Fabrocini (1988)
UV <sub>14</sub> +TNI	p, n, e <sup>-</sup> , μ <sup>-</sup>	Urbana V <sub>14</sub> and TNI	NRV	Wiringa et al. (1988)
TF	p, n, e <sup>-</sup> , μ <sup>-</sup>	TF96	Thomas-Fermi model	Strobel et al. (1997)
HV <sub>pn</sub>	p, n, e <sup>-</sup> , μ <sup>-</sup>	exchange of σ, ω, ρ	RH	Weber & Weigel (1989)
HV	p, n, Λ, Σ <sup>±,0</sup> , Ξ <sup>0,-</sup> , e <sup>-</sup> , μ <sup>-</sup>	exchange of σ, ω, ρ	RH	Weber & Weigel (1989)
RH1	p, n, Λ, Σ <sup>±,0</sup> , Ξ <sup>0,-</sup> , Δ <sup>-,0,+</sup> , ++, e <sup>-</sup> , μ <sup>-</sup>	exchange of σ, ω, π, ρ	RBHF+RH	Huber et al. (1998)
RHF <sub>pn</sub>	p, n, e <sup>-</sup> , μ <sup>-</sup>	exchange of σ, ω, π, ρ	RBHF+RH	Huber et al. (1998)
RHF1	p, n, Λ, Σ <sup>±,0</sup> , Ξ <sup>0,-</sup> , Δ <sup>-,0,+</sup> , ++, e <sup>-</sup> , μ <sup>-</sup>	exchange of σ, ω, π, ρ	RBHF+RHF	Huber et al. (1998)
RHF8	p, n, Λ, Σ <sup>±,0</sup> , Ξ <sup>0,-</sup> , Δ <sup>-,0,+</sup> , ++, e <sup>-</sup> , μ <sup>-</sup>	exchange of σ, ω, π, ρ	RBHF+RHF	Huber et al. (1998)
G <sub>300</sub>	p, n, Λ, Σ <sup>±,0</sup> , Ξ <sup>0,-</sup> , e <sup>-</sup> , μ <sup>-</sup>	exchange of σ, ω, ρ	RH	Glendenning (1989)
G <sub>300</sub> <sup>π</sup>	p, n, Λ, Σ <sup>±,0</sup> , Ξ <sup>0,-</sup> , e <sup>-</sup> , μ <sup>-</sup> , π-condensation	exchange of σ, ω, ρ	RH	Glendenning (1989)
G <sub>K240</sub>	p, n, e <sup>-</sup> , μ <sup>-</sup>	exchange of σ, ω, ρ	RH	Glendenning (1995)
G <sub>pn</sub> <sup>K240</sup>	p, n, Λ, Σ <sup>±,0</sup> , Ξ <sup>0,-</sup> , e <sup>-</sup> , μ <sup>-</sup>	exchange of σ, ω, ρ	RH	Glendenning (1997)
G <sub>M78</sub> <sup>K240</sup>	p, n, Λ, Σ <sup>±,0</sup> , Ξ <sup>0,-</sup> , e <sup>-</sup> , μ <sup>-</sup>	exchange of σ, ω, ρ	RH	Glendenning (1995)
G <sub>M78</sub> <sup>K240</sup>	p, n, Λ, Σ <sup>±,0</sup> , Ξ <sup>0,-</sup> , e <sup>-</sup> , μ <sup>-</sup>	exchange of σ, ω, ρ	RH	Glendenning (1995)
G <sub>K240</sub> <sup>M78</sup>	p, n, Λ, Σ <sup>±,0</sup> , Ξ <sup>0,-</sup> , e <sup>-</sup> , μ <sup>-</sup> , quarks	exchange of σ, ω, ρ	RH	Glendenning (1997)
G <sub>B180</sub>	p, n, Λ, Σ <sup>±,0</sup> , Ξ <sup>0,-</sup> , e <sup>-</sup> , μ <sup>-</sup>	exchange of σ, ω, ρ, φ	RH	Schaffner & Mishustin (1996)
TM1-m1	p, n, Λ, Σ <sup>±,0</sup> , Ξ <sup>0,-</sup> , e <sup>-</sup> , μ <sup>-</sup>	exchange of σ, ω, ρ, σ*, φ	RH	Schaffner & Mishustin (1996)
TM1-m2	p, n, Λ, Σ <sup>±,0</sup> , Ξ <sup>0,-</sup> , e <sup>-</sup> , μ <sup>-</sup>	exchange of σ, ω, ρ, σ*, φ	RH	Schaffner & Mishustin (1996)
NLSH1	p, n, Λ, Σ <sup>±,0</sup> , Ξ <sup>0,-</sup> , e <sup>-</sup> , μ <sup>-</sup>	exchange of σ, ω, ρ, φ	RH	Schaffner & Mishustin (1996)
NLSH2	p, n, Λ, Σ <sup>±,0</sup> , Ξ <sup>0,-</sup> , e <sup>-</sup> , μ <sup>-</sup>	exchange of σ, ω, ρ, σ*, φ	RH	Schaffner & Mishustin (1996)
SM <sub>B145</sub>	u, d, s	Bag model	Fermi gas	Farhi & Jaffe (1984)
SM <sub>B160</sub>	u, d, s	Bag model	Fermi gas	Farhi & Jaffe (1984)

Abbreviations: NRV=non-relativistic variational method, RH=relativistic Hartree approximation, RHF=relativistic Hartree-Fock approximation, RBHF=relativistic Brückner-Hartree-Fock approximation.


**Figure 1.** Pressure-density relation for several EOSs

(1984). If the hypothesis is true, then a separate class of compact stars could exist, which range from dense strange stars to strange dwarfs to strange planets (Weber et al., 1995; Glendenning et al., 1995b; Glendenning et al., 1995a). In principle both strange and neutron stars could exist. However if strange stars exist, the galaxy is likely to be contaminated by strange quark nuggets which would convert via impact “conventional” neutron stars into strange stars (Glendenning, 1990; Madsen & Olesen, 1991; Caldwell & Friedman, 1991). This would imply that the objects known to astronomers as pulsars are probably rotating strange matter stars and not neutron matter stars, as it is usually assumed. Presently there is no sound scientific basis on which one can either confirm or reject the hypothesis, so that it remains a serious possibility of fundamental significance for compact stars (Weber et al., 1997b; Weber et al., 1997a; Madsen,

1998) plus various other physical phenomena (Madsen & Haensel, 1991). Below we will explore the implications of the existence of strange stars with respect to the QPO phenomena. This enables one to test the possible existence of strange stars and thus draw definitive conclusions about the true ground state of strongly interacting matter.

As pointed out by Alcock et al. (1986), a strange star can carry a solid nuclear crust whose density is strictly limited by neutron drip. This possibility is caused by the displacement of electrons at the surface of the strange matter core, which generates an electric dipole layer there. It can be sufficiently strong to produce a gap between ordinary atomic matter (crust) and the quark-matter surface, which prevents a conversion of ordinary atomic matter into the assumed lower-lying ground state of strange matter. Obviously, free neutrons, being electrically charge neutral, cannot exist in the crust, because they do not feel the Coulomb barrier and thus would gravitate toward the strange-quark matter core, where they are converted by hypothesis into strange matter. Consequently, the density at the base of the crust (inner crust density) must always be smaller than neutron drip density. The situation is illustrated in Fig. 2 where the EOS of a strange star with crust is shown.

The strange-star models presented in the following are constructed for an EOS of strange matter derived by Farhi & Jaffe (1984). We shall study models with a fixed strange quark mass,  $m_s = 100$  MeV, and the two bag constants,  $B^{1/4} = 145$  MeV and  $B^{1/4} = 158$  MeV.

#### 4 KILOHERTZ QUASI PERIODIC OSCILLATIONS

In Table 2 the observations of kilohertz QPOs from 16 sources are summarised. The sources can be classified into two classes, the Atoll- and the Z-sources, depending on the form of their colour-colour diagram. Almost all sources show

**Table 2.** Observational data of kilohertz QPOs

Source	Type	$\nu_{\text{QPO1}}$ [Hz]	$\nu_{\text{QPO2}}$ [Hz]	$\Delta\nu_{\text{QPO1}}$ [Hz]	$\nu_{\text{Burst}}$ [Hz]	References
4U 0614+091	Atoll	750–1145 $\pm$ 10	480–800	323 $\pm$ 4	328 $\ddagger$	1
4U 1608-52 $\ddagger$	Atoll	940–1125	650–890	233 $\pm$ 12–293 $\pm$ 7		2,3,4,5,6
4U 1636-536 $\ddagger$	Atoll	1147–1228	830–940	257 $\pm$ 20–276 $\pm$ 10	581	6,7,8
4U 1728-34	Atoll	988–1058 $\pm$ 12	638–716	355 $\pm$ 5	363	7,9
KS 1731-260	Atoll	1176–1197 $\pm$ 10	900	260 $\pm$ 10	523.92 $\pm$ 0.05	10,11
4U 1735-44	Atoll	982–1161 $\pm$ 1	632–729	296 $\pm$ 12–341 $\pm$ 7		12,13
4U 1820-30 $\ddagger$	Atoll	640–1060 $\pm$ 20	400–800	275 $\pm$ 8		14
Aql X-1	Atoll	740–830			549	15
GX 3+1	Atoll					16
4U 1705-44	Atoll	1074 $\pm$ 10	776–867	298 $\pm$ 11		17
Sco X-1	Z	872–1115	565–890	310–230		18
GX 5-1	Z	567–895	325–448	298 $\pm$ 11		19
GX 17+2	Z	645–1087 $\pm$ 12	480–781	294 $\pm$ 8		20
Cyg X-2	Z	731–1007 $\pm$ 12	490–780	346 $\pm$ 29		21
GX 349+2	Z	978 $\pm$ 9	712	266 $\pm$ 13		22
GX 340+0	Z	567–820 $\pm$ 19	247–625	325 $\pm$ 10		23

$\ddagger$ : QPO is statistical not significant,  $\ddagger$ :  $\nu_{\text{QPO1}}^{\text{max}}$  is independent of luminosity. References 1: Ford et al. (1997), 2: Méndez et al. (1998a), 3: Méndez et al. (1998b), 4: Yu et al. (1997a), 5: Yu et al. (1997b), 6: Kaaret et al. (1997), 7: van der Klis (1998), 8: Strohmayer et al. (1998), 9: Strohmayer et al. (1996), 10: Wijnands & van der Klis (1997), 11: Smith, Morgan & Bradt (1997), 12: Wijnands et al. (1998c), 13: Ford et al. (1998b), 14: Zhang et al. (1998b), 15: Zhang et al. (1998a), 16: Strohmayer (1998), 17: Ford, van der Klis & Kaaret (1998a), 18: van der Klis & Wijnands (1997), 19: Wijnands et al. (1998b), 20: Wijnands et al. (1997), 21: Wijnands et al. (1998a), 22: Zhang, Strohmayer & Swank (1998c), 23: Jonker et al. (1998)

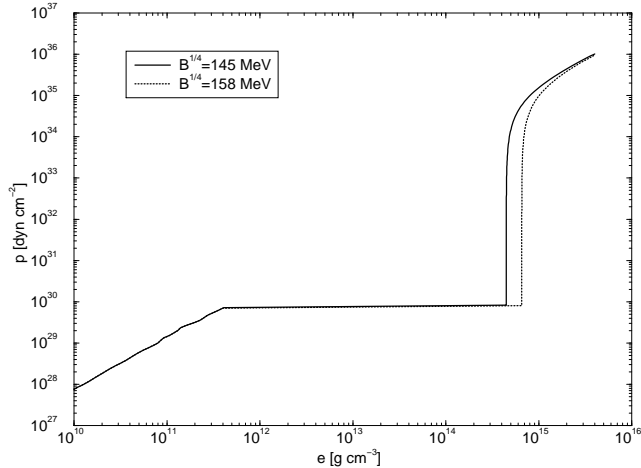


**Figure 2.** Pressure-density relation for strange stars with crust. The bag constant is  $B^{1/4} = 145$  MeV or 158 MeV, respectively, the mass of the strange quark is  $m_s = 100$  MeV.

simultaneously two kilohertz QPOs. Although the frequencies of both QPOs vary by several hundred Hertz with the accretion rate, the variation of the frequency separation is only small.

Therefore the observations strongly favour some kind of beat-frequency model. In such models the upper kilohertz QPO corresponds to the Kepler rotation at the inner edge of the accretion disk. The lower QPO corresponds to the beat frequency between the upper QPO and the spin of the neutron star. This interpretation is supported by the fact that the frequency separation is equal to the QPO frequency (or half of it) in type I X-ray bursts observed in some of the Atoll

sources (see Tab. 2). The question remains however where the upper QPO is generated. Strohmayer et al. (1996) suggested that this radius is identical to the magnetospheric radius, whereas Miller et al. (1998c) propose that it is identical to the sonic radius (see van der Klis 1997 for a critical discussion of these models). In both cases, the orbital radius has to be larger than the radius of the innermost stable orbit (see Sect. 2.2), or equivalently, the frequency  $\nu_{\text{QPO1}}$  of the upper QPO has to be smaller than the Kepler frequency at the innermost stable orbit:

$$\nu_{\text{QPO1}} \leq \nu_{\text{K}}^{\text{ms}} \approx 2200 \frac{M_{\odot}}{M} \text{ Hz}, \quad (21)$$

where the approximate expression (19) was used. The exact expression depends on the EOS and on the spin period of the neutron star. This inequality sets an upper limit to the mass of the star. Obviously, the orbital radius has to be larger than the star's radius, which is larger than the radius of the innermost stable orbit for low star masses. This constraint sets a lower limit to the star mass which again depends on the spin period and the EOS.

Figure 3 shows the maximally allowed Kepler frequency as function of the gravitational mass for two EOSs, RHF<sub>pn</sub> and RHF8. If the radius of the innermost stable orbit is smaller than the star's radius the maximally allowed Kepler frequency is given by the Kepler frequency at the star's equator. This kind of solution is represented by the rising branch of  $\nu_{\text{K}}(M)$ , since  $\nu_{\text{K}}$  increases with increasing gravitational mass. If the innermost stable orbit is located outside the star the maximally allowed Kepler frequency decreases again with increasing mass. The two EOSs differ for  $M \gtrsim 1.0 M_{\odot}$  in the composition. In RHF8 hyperons are included, whereas RHF<sub>pn</sub> assumes pure nucleonic matter. RHF8 is therefore softer than RHF<sub>pn</sub> at high densities. This means also, that

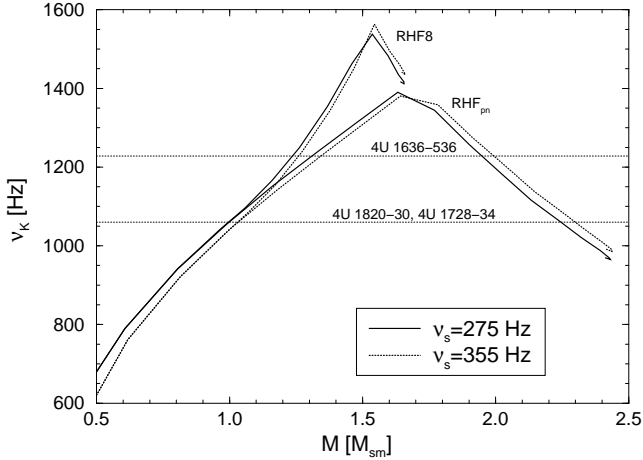


**Figure 3.** Maximally allowed Kepler frequency  $\nu_K$  as function of the neutron star’s mass  $M$  for the two EOSs RHF<sub>pn</sub> and RHF8 and two different spin frequencies  $\nu_s = 275$  and  $355$  Hz.

RHF8 can only support smaller masses than RHF<sub>pn</sub>. The maximally allowed Kepler frequency depends only slightly on the neutron star’s spin frequency, as long as the spin frequency is not larger than about ten percent of the star’s Kepler frequency. If one compares the  $\nu_K$ -curves for example with the frequency  $\nu_{\text{QPO1}}^{\text{max}} = 1060$  of the highest kilohertz QPO observed in 4U 1820-30 ( $\nu_s = 275$  Hz), one obtains that the mass of the neutron star has to be within the range between  $M = 1.0 M_\odot$  and  $2.25 M_\odot$  (for RHF<sub>pn</sub>) and  $M_{\text{max}} = 1.65 M_\odot$  (for RHF8), respectively.

If one adopts the interpretation of the sonic-point model one expects that the inner boundary of the accretion disc is close to the innermost stable orbit. Indeed, the observations of the sources 4U 1820-30, 4U 1608-52, and 4U 1636-536 seem to confirm this interpretation, since the QPO frequency remains constant for high mass accretion rates (Kaaret et al., 1997; Zhang et al., 1998b). Therefore, only the right intersection point of the  $\nu_K(M)$ -curve with the line  $\nu_K = \nu_{\text{QPO1}}^{\text{max}}$  is allowed by the observations<sup>†</sup>. The mass of the neutron star in the binary system 4U 1820-30 can now be determined. For RHF<sub>pn</sub> the mass is equal to  $M = 2.25 M_\odot$  whereas RHF8 would be excluded.

The figures 4–6 show the respective ranges of masses for which the Kepler frequency at the equator or at the innermost stable orbit is larger than the highest observed QPO frequency  $\nu_{\text{QPO1}}^{\text{max}}$  for all EOSs considered here (see Tab. 1). The vertical line refers to the approximate mass, which is obtained by setting  $j = 0$  in Eq. (19). This expression underestimated the upper limit of the mass. The dashed bars refer to the EOSs for which models with  $\nu_K^{\text{ms}} = \nu_{\text{QPO1}}^{\text{max}}$  do not exist, i.e. whose maximally stable mass is too small. If the interpretation of the highest observed QPO frequency in the three sources 4U 1820-30, 4U 1608-52, and 4U 1636-536 is confirmed, the mass of the neutron star is constrained to

<sup>†</sup> The left intersection point is unlikely, since it is expected that the lower and the upper frequency QPO cannot be observed at the same time if the accretion disk would extend to the neutron star surface (Zhang et al., 1997). This would be contrary to the simultaneous observation of both QPOs in several sources.

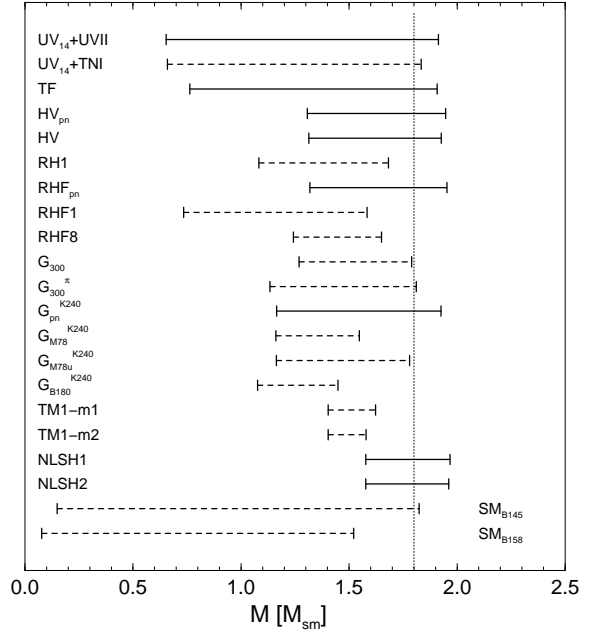


**Figure 4.** Range of masses for which the Kepler frequency at the equator or at the innermost stable orbit is larger than the highest observed QPO frequency  $\nu_{\text{QPO1}}^{\text{max}} = 1228$  Hz in the source 4U 1636-536 ( $\nu_s = 290$  Hz). The dashed bars refer to the EOSs for which models with  $\nu_K^{\text{ms}} = \nu_{\text{QPO1}}^{\text{max}}$  do not exist. The approximate value  $M_{\text{appr}} = 1.80 M_\odot$  is also shown.

the respective right end of the solid bars. The EOSs, for which models with  $\nu_K^{\text{ms}} = \nu_{\text{QPO1}}^{\text{max}}$  do not exist (dashed bars) are excluded.

Especially, the observation of 4U 1820-30 agrees only with the two nucleonic EOSs UV<sub>14</sub>+UVII and RHF<sub>pn</sub>. If the interpretation of the highest observed QPO frequency in this source is confirmed by further observations, the existence of hyperons, meson condensates, quark condensates, and strange stars can be rejected. The neutron star matter consists thus only of nucleons and leptons. At least, the hyperon fraction (i.e. strangeness) is much smaller than predicted by actual relativistic calculations.

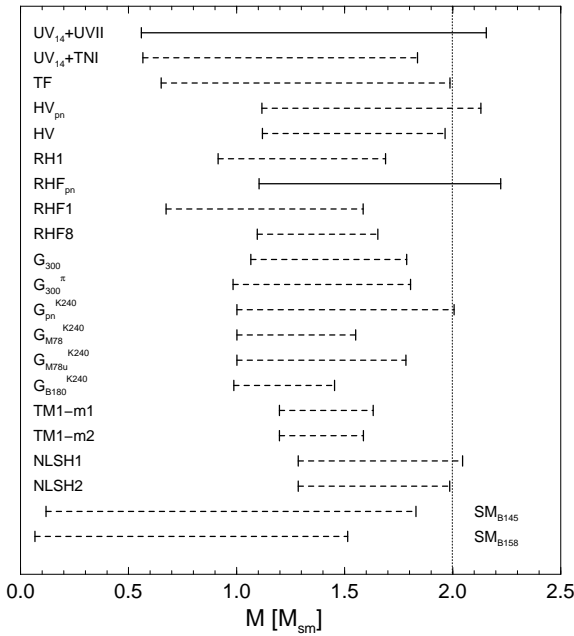
Figures 7 and 8 show the allowed ranges of mass of the neutron stars in the respective binaries for the EOSs RHF<sub>pn</sub> and RHF8, respectively. For RHF8, the masses are limited by the maximally stable star mass  $M_{\text{max}} \sim 1.65 M_\odot$ , which depends on the spin period. All sources are consistent with a canonical star mass of  $M = 1.4 M_\odot$ . Only if one assumes that the highest QPO frequency is equal to the Kepler frequency at the innermost stable orbit, the masses lie between  $M = 2.0 M_\odot$  and  $2.5 M_\odot$  (for RHF<sub>pn</sub>).

## 5 CONSTRAINTS ON EQUATION OF STATE BY LENSE-THIRRING PRECESSION

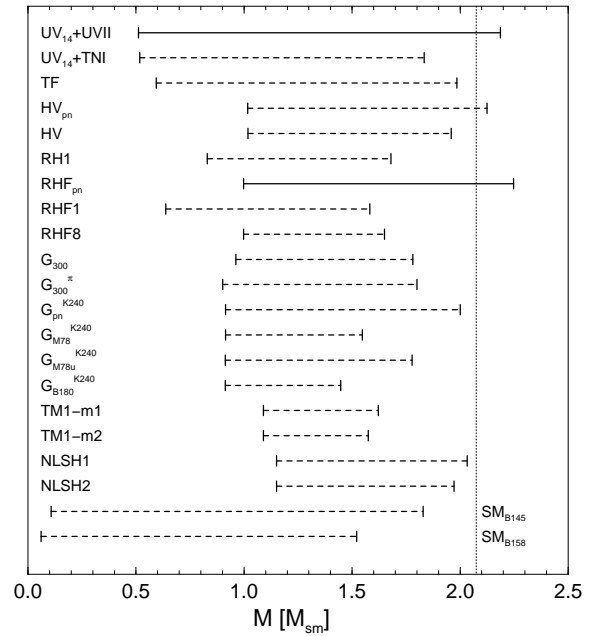
Stella & Vietri (1998) suggested that a third oscillation with a frequency  $\nu_{\text{QPO3}}$  around  $\sim 10$  Hz is also produced at the inner border of the accretion disk by Lense-Thirring precession. The observed frequencies  $\nu_{\text{QPO3}}$  (s. Tab. 3) can again be compared with theoretical neutron star models. The neutron star models are constructed for a given spin

**Table 3.** Observational data of QPOs in the 10 Hz range.

Source	$\nu_s$ [Hz]	$\nu_K$ [Hz]	$\nu_{\text{QPO3}}$ [Hz]	References
4U 0641+91	323	900	22	Stella & Vietri (1998)
4U 1608-52	233	800	20	Yu et al. (1997a)
4U 1728-34	355	355	9.0	Ford & van der Klis (1998)
		551	14.1	
		699	26.5	
		1122	41.5	
KS 1731-260	262	1197	27	Wijnands & van der Klis (1997)
4U 1735-44	326	1149	29	Wijnands et al. (1998c)
Sco X-1	247	1050	5	van der Klis (1996)
		1101	9	
		1135	13	
GX 17+2	294	644	5	Wijnands et al. (1997)
		832	9	
		1042	13	
Cyg X-2	346	731	5	Wijnands et al. (1998a)
		856	9	
		1007	13	
GX 340+0	325	569	5	Jonker et al. (1998)
		730	9	
		823	13	
GX 5-1	298	506	5	Wijnands et al. (1998b)
		685	9	
		889	13	

**Figure 5.** Same as in Fig. 4 but for the source 4U 1728-34 ( $\nu_{\text{QPO1}}^{\text{max}} = 1100$  Hz,  $\nu_s = 355$  Hz,  $M_{\text{appr}} = 2.01M_{\odot}$ ).

frequency  $\nu_s$  and a fixed, unfortunately unknown, star mass  $M$ . The obtained monotone relations  $\nu_K(r, \theta = \pi/2)$  and  $\nu_{\text{LT}}(r, \theta = \pi/2)$  are transformed into the relation  $\nu_{\text{LT}}(\nu_K)$ .

**Figure 6.** Same as in Fig. 4 but for the source 4U 1820-30 ( $\nu_{\text{QPO1}}^{\text{max}} = 1060$  Hz,  $\nu_s = 275$  Hz,  $M_{\text{appr}} = 2.07M_{\odot}$ ).

Since the Lense-Thirring precession frequency  $\nu_{\text{LT}}$  is, in first approximation, proportional to  $\nu_s$  the relation  $\nu_{\text{LT}}/\nu_s$  as function of  $\nu_K$  is shown in Fig. 9 for all EOSs. The observa-



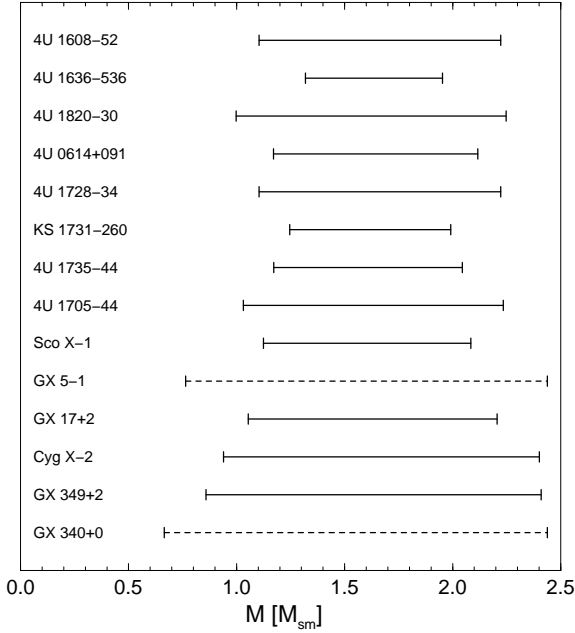


**Figure 7.** Same as in Fig. 4 but for different sources and the fixed EOS RHF<sub>pn</sub>.

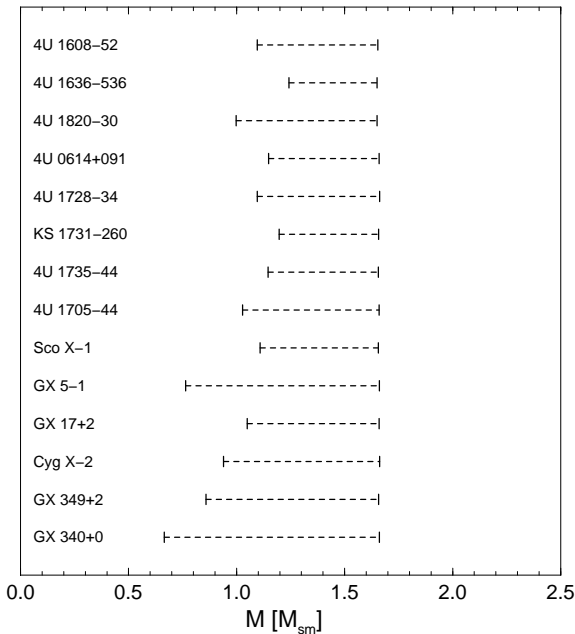


**Figure 8.** Same as in Fig. 7 but for RHF8.

tions are shown as circles. The curves depend only weakly on the neutron star mass. One can therefore draw conclusions from the comparison of the theoretical curves with the observations, although the star masses are unknown. Since both  $\nu_{LT}/\nu_s$  and  $\nu_K$  do not depend on  $\nu_s$  in first approximation, the calculation of the theoretical curves for one specific spin frequency,  $\nu_s = 363$  Hz (this corresponds to the spin frequency of the neutron star in 4U1728-34), is sufficient.

As can be seen in Fig. 9, the observations of KS 1731-260 and 4U 1735-44 agree with the theoretical curves of group 1, which contains the stiffest EOSs of our sample. This is in

agreement with the results of Stella & Vietri (1998). However, the other observations, including the observations of the Z-sources which are not shown, lie above all theoretical curves. The observed frequency  $\nu_{QPO3}$  is thus higher than the Lense-Thirring precession frequency even for the stiffest EOSs. If one assume that the observed frequencies correspond to the first overtone of the Lense-Thirring precession, the Atoll-source observations are in the range of the theoretical curves.

In the case of the Z-sources, the detected frequencies  $\nu_{QPO3}$  are not only too large in most sources, but additionally the slope of the relation  $\nu_{QPO3}(\nu_{QPO1})$  of the Z-source observations is much higher than the slope of  $\nu_{LT}(\nu_K)$  for the theoretically determined models. Even the assumption, that the first overtone of the Lense-Thirring precession frequency  $\nu_{LT}$  is detected (Stella & Vietri, 1998) cannot explain these discrepancies.

## 6 CONCLUSIONS

In this paper, we derived models of rapidly rotating neutron stars and strange stars by solving the general relativistic structure equations for a broad collection of modern EOSs. We compared the space time geometry of these models with recently discovered QPOs in the X-ray brightness of LMXBs.

If one follows the general beat-frequency interpretation of the kilohertz-QPOs, i.e. that the higher frequency QPO originates at a stable circular orbit, one can constrain the mass of the neutron star to a range which depends on the EOS. This mass range is for all sources and for all EOSs consistent with a canonical mass,  $M = 1.4 M_\odot$ . As it was stated by Miller et al. (1998a) and Thampan et al. (1999) the exact lower and upper limits of the neutron star's mass can only be determined by using fully relativistic models of rapidly rotating neutron stars. The exact limits differ from the approximations with  $j = 0$  by roughly 10 %.

As it was shown by Kaaret et al. (1997) and Zhang et al. (1998b), the observation of a maximum frequency  $\nu_{QPO1}^{\max}$  of the high frequency QPO in the sources 4U 1820-30, 4U1608-52, and 4U 1636-536 favour the interpretation that this QPO originates at the innermost stable orbit. If this interpretation is correct, the mass of the neutron star can be exactly (within the observational errors) determined for a given EOS. The approximately obtained mass,  $M = 2.07 M_\odot$ , of the source 4U 1820-30 is larger than the maximum mass of most of the considered EOSs. This conclusion is even strengthened if the observed maximum frequency  $\nu_{QPO1}^{\max}$  is compared with the exact neutron star models. The only allowed EOSs of our broad collection are then the UV<sub>14</sub>+UVII and RHF<sub>pn</sub>, which both describe neutron star matter as consisting of nucleons and leptons only. The derived masses of the three sources lie in the narrow range between  $M = 1.92 M_\odot$  and  $2.25 M_\odot$ .

This result is also of some importance for the nature of the object left in the supernova 1987A. During the first ten seconds after the supernova, neutrinos were detected (Chevalier, 1997). This means that a protoneutron star was formed in the supernova. The fact that up to now no pulsar emission could be detected was interpreted by Bethe & Brown (1995) that the protoneutron star collapsed to a black hole when the star became transparent to neutrinos

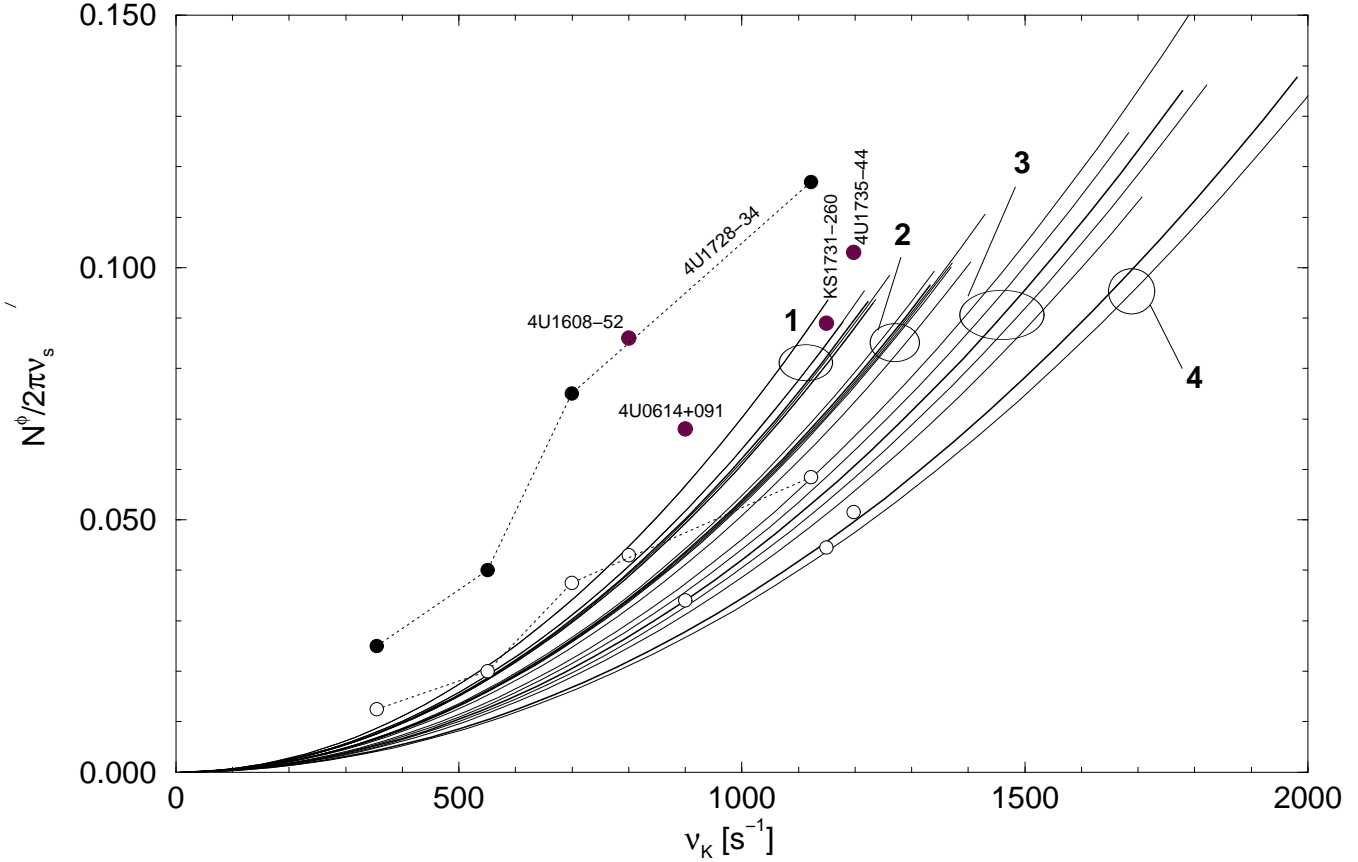


**Figure 9.** Ratio  $\nu_{\text{LT}}/\nu_s$  of the Lense-Thirring precession frequency  $\nu_{\text{LT}}$  and the spin frequency  $\nu_s \equiv 363$  Hz as function of the Kepler frequency  $\nu_K$ . The used mass is  $M = 1.4M_\odot$ . The first group of curves contains the EOSs: NLSH1, NLSH2, TM1-m2, TM1-m1, **RHF**<sub>pn</sub>, G<sub>300</sub>, HV<sub>pn</sub>, and HV (from the left to the right; the bold typed label corresponds to the bold curve). Group 2: G<sub>pn</sub><sup>K240</sup>, **RHF8**, RH1, G<sub>300</sub><sup>pi</sup>, G<sub>M78u</sub><sup>K240</sup>, and G<sub>M78</sub><sup>K240</sup>. Group 3: SM<sub>B145</sub>, TF, **UV**<sub>14</sub>+**UVII**, UV<sub>14</sub>+TNI, and G<sub>B180</sub><sup>K240</sup>. Group 4: **RHF1** and SM<sub>B160</sub>. The full (open) circles correspond to (half of) the observations of the Atoll-sources in Tab. 3.

after roughly 10 s. The estimated value of the baryonic mass  $M_B \sim 1.63 - 1.76 M_\odot$  (Bethe & Brown, 1995; Thielemann et al., 1996) gives thus an upper limit to the maximum gravitational mass of a neutron star:  $M_{\text{max}} \lesssim 1.6 M_\odot$ . This limit is in clear contradiction to the derived mass of, e.g. 4U 1820-30.

It is generally believed that neutron stars are born with a mass about  $1.4 - 1.5 M_\odot$ . Neutron stars in LMXBs would therefore accrete  $0.4 - 0.8 M_\odot$  during their lifetime. It seems reasonable to assume that some of the neutron stars in LMXBs accrete enough matter to reach the maximally stable mass ( $M_{\text{max}} = 2.20 M_\odot$  for UV<sub>14</sub>+UVII,  $M_{\text{max}} = 2.44 M_\odot$  for RHF<sub>pn</sub>). The neutron star would then collapse to a black hole.

The interpretation of the QPO with frequencies  $\nu_{\text{QPO3}}$  about 10 Hz as Lense-Thirring precession frequency of the accretion disk seems not to be consistent with the theoretical star models, unless one assumes that the first overtone of the precession is observed. In the case of Z-sources however, the necessary ratio of the frame dragging frequency and spin frequency, and thus the moment of inertia, of the models if too small compared to the observed frequency  $\nu_{\text{QPO3}}$  or half of it.

Our general conclusion is that the observations of kilohertz QPOs in LMXBs provide us another powerful tool for

probing the interior of neutron stars. Compared to the other tools like observations of the maximum mass (van Kerkwijk et al., 1995), the limiting spin period (Friedman et al., 1986; Weber & Glendenning, 1992), and cooling simulations (Tsuruta, 1966; Schaab et al., 1996; Page, 1998), the derived constraints, especially in the sonic-point-interpretation, are rather strong. The lower limit  $M_{\text{max}} \gtrsim 2.15 M_\odot$  is only consistent with two EOSs, UV<sub>14</sub>+UVII and RHF<sub>pn</sub>, which are relatively stiff at high densities. Their stiff behaviour at high densities seems to be only possible if the neutron star matter consists of neutrons, protons, and leptons only. At the most, a small admixture of hyperons may be allowed. However, one has to admit that such a composition somehow contradicts our conception of neutron star matter, since fieldtheoretical models lead more or less inevitably to a more complex composition at high density. If the given interpretation is correct, one has therefore to reinvestigate the problem of super dense neutron star matter by dropping, for instance, the standard assumptions about the coupling of the hyperons in such regimes.

This specific conclusion depends however on the interpretation of the maximum frequency of the kilohertz QPO within the sonic-point-model. As a kind of beat-frequency model, this model predicts a constant frequency separation  $\Delta\nu = \nu_{\text{QPO1}} - \nu_{\text{QPO2}}$ . Recently two further exam-

ples, where this constancy is not observed, has been discovered: 4U 1608-52 and 4U 1735-44 (Méndez et al., 1998; Ford et al., 1998b). Moreover, the frequency separation in the Atoll source 4U 1636-536 seems not to be consistent with the half of the frequency of the QPO in type I bursts (Méndez & van Paradijs, 1998). Though the beat-frequency models are the most hopeful candidates in explaining the QPO-phenomenology it has to be awaited how the variation of the frequency separation and deviation from the QPO frequency in bursts can be incorporated to these models.

## ACKNOWLEDGEMENTS

One of us (Ch. S.) gratefully acknowledges the Bavarian State for financial support. We would like to thank Norman Glendenning and Jürgen Schaffner-Bielich for providing us tables of their EOSs.

## REFERENCES

- Alcock C., Farhi E., Olinto A.V., 1986, ApJ, 310, 261  
 Balberg S., Gal A., 1997, Nucl. Phys. A, 625, 435  
 Balberg S., Lichtenstadt I., Cook G.B., 1998, Roles of hyperons in neutron stars, to be published in ApJS, preprint astro-ph/9810361  
 Batty C.J., Friedman E., Gal A., 1994, Phys. Lett. B, 335, 273  
 Bethe H.A., Brown G.E., 1995, ApJ, 445, L129  
 Bodmer A., 1971, Phys. Rev. D, 4, 1601  
 Bonazzola S., Gourgoulhon E., Sagado M., Marck J., 1993, A&A, 278, 421  
 Börner G., 1973, in *Ergebnisse der exakten Naturwissenschaften, Band 69*, Springer, Berlin, pp. 1–67  
 Caldwell R., Friedman J., 1991, Phys. Lett., 264B, 143  
 Chevalier R.A., 1997, Sci, 276, 1374  
 Cook G.B., Shapiro S.L., Teukolsky S.A., 1992, ApJ, 398, 203  
 Datta B., Thampan A.V., Bombacci I., 1998, A&A, 334, 943  
 Farhi E., Jaffe R., 1984, Phys. Rev. D, 30, 2379  
 Ford E., Kaaret P., Tavani M., Barret D., Bloser P., Grindlay J., Harmon B.A., Paciesas W.S., Zhang S.N., 1997, ApJ, 475, L123  
 Ford E.C., van der Klis M., 1998, ApJ, 506, L39  
 Ford E.C., van der Klis M., Kaaret P., 1998a, ApJ, 498, L41  
 Ford E.C., van der Klis M., Méndez M., Wijnands R., Kaaret P., 1998b, ApJ, 508, L155  
 Friedman J.L., Ipser J.R., Parker L., 1986, ApJ, 304, 115  
 Glendenning N.K., 1989, Nucl. Phys. A, 493, 521  
 Glendenning N.K., 1990, Mod. Phys. Lett., A5, 2197  
 Glendenning N.K., 1995, unpublished  
 Glendenning N.K., 1997, Compact Stars: Nuclear Physics, Particle Physics and General Relativity, Springer, New-York  
 Glendenning N.K., Kettner C., Weber F., 1995a, Phys. Rev. C, 51, 1790  
 Glendenning N.K., Kettner C., Weber F., 1995b, Astrophysical Journal, 450, 253  
 Haensel P., Pichon B., 1994, A&A, 283, 313  
 Huber H., 1998, Ph.D. thesis, University of Munich, unpublished  
 Huber H., Weber F., Weigel M.K., Schaab C., 1998, Int. J. Mod. Phys. E, 7, 301  
 Jonker P.G., Wijnands R., van der Klis M., Psaltis D., Kuulkers E., Lamb F.K., 1998, ApJ, 499, L191  
 Kaaret P.K., Ford E., Chen K., 1997, ApJ, 480, L27  
 Lamb F.K., Miller M.C., Psaltis D., 1998, in *Accretion Processes in Astrophysical Systems: Some Like It Hot*, AIP Conference Proceedings 431  
 Lense J., Thirring H., 1918, Phys. Z., 19, 156  
 Madsen J., 1998, How to identify a strange star, astro-ph/9806032  
 Madsen J., Haensel P., eds., 1991, Strange Quark Matter in Physics and Astrophysics, Proceedings of the International Workshop, Aarhus, Denmark, vol. 24  
 Madsen J., Olesen M.L., 1991, Phys. Rev. D, 43, 1069, erratum: ibid. D44 (1991) 566  
 Méndez M., van Paradijs J., 1998, Difference frequency of kilohertz qpos is not equal to half the burst oscillation frequency in 4u 1636-53, astro-ph/9808281  
 Méndez M., van der Klis M., van Paradijs J., Lewin W.H.G., Vaughan B.A., Kuulkers E., Zhang W., Lamb F.K., Psaltis D., 1998a, in *Accretion Processes in Astrophysical Systems: Some Like It Hot*, AIP Conference Proceedings 431  
 Méndez M., van der Klis M., van Paradijs J., Lewin W.H.G., Vaughan B.A., Kuulkers E., Zhang W., Lamb F.K., Psaltis D., 1998b, ApJ, 494, L65  
 Méndez M., van der Klis M., Wijnands R., Ford E.C., van Paradijs J., Vaughan B.A., 1998c, ApJ, 505, L23  
 Miller M.C., 1998, Evidence for antipodal hot spots during x-ray bursts from 4U 1636-536, astro-ph/9809235  
 Miller M.C., Lamb F.K., Cook G.B., 1998a, ApJ, 509, 793, submitted to ApJ, preprint astro-ph/9805007  
 Miller M.C., Lamb F.K., Psaltis D., 1998b, in Scarsi L., Bradt H., Giommi P., Fiore F., eds., *The Active X-Ray Sky: Results from BeppoSAX and RXTE*, Elsevier (Amsterdam), Nucl. Phys. B 69  
 Miller M.C., Lamb F.K., Psaltis D., 1998c, ApJ, 508, 791  
 Misner C.W., Thorne K.S., Wheeler J.A., 1973, Gravitation, W.H. Freeman and Company, New York  
 Myers W.D., Swiatecki W.J., 1996, Nucl. Phys. A, 601, 141  
 Negele J., Vautherin D., 1973, Nucl. Phys. A, 207, 298  
 Page D., 1998, in Buccheri R., van Paradijs J., Alpar A., eds., *The Many Faces of Neutron Stars*, Kluwer (Dordrecht)  
 Pethick C., Ravenhall P., Lorenz C., 1995, Nucl. Phys. A, 584, 675  
 Psaltis D., Méndez M., Wijnands R., Homan J., Jonker P.G., van der Klis M., Lamb F.K., Kuulkers E., van Paradijs J., Lewin W.H.G., 1998, ApJ, 501, L95  
 Schaab C., 1999, Struktur und Thermische Entwicklung von Neutronensternen und Strange Sternen, GCA-Verlag (Herdecke), ISBN 3-928973-53-3, PhD-Thesis  
 Schaab C., Weber F., Weigel M.K., Glendenning N.K., 1996, Nucl. Phys. A, 605, 531  
 Schaffner J., Mishustin I.N., 1996, Phys. Rev. C, 53, 1416  
 Smarr L., York J.W., 1978, Phys. Rev. D, 17, 2529  
 Smith D.A., Morgan E.H., Bradt H., 1997, ApJ, 479, L137  
 Stella L., Vietri M., 1998, ApJ, 492, L59  
 Strobel K., Weber F., Schaab C., Weigel M.K., 1997, Int. J. Mod. Phys. E, 6, 669  
 Strohmayer T.E., 1998, in *Accretion Processes in Astrophysical Systems: Some Like It Hot*, AIP Conference Proceedings 431  
 Strohmayer T.E., Zhang W., Swank J.H., Smale A., Titarchuk L., Day C., 1996, ApJ, 469, L9  
 Strohmayer T.E., Zhang W., Swank J.H., White N.E., 1998, ApJ, 498, L135  
 Thampan A.V., Bhattacharya D., Datta B., 1999, MNRAS, 302, L69  
 Thielemann F.K., Nomoto K., Hashimoto M., 1996, ApJ, 460, 408  
 Tsuruta S., 1966, Canadian Journal of Physics, 44, 1863  
 van der Klis M., 1998, in Buccheri R., van Paradijs J., Alpar A., eds., *The Many Faces of Neutron Stars*, Kluwer (Dordrecht)  
 van der Klis M., Wijnands R.A.D., 1997, ApJ, 481, L97  
 van der Klis M., Swank J.H., Zhang W., Jahoda K., Morgan E.H., Lewin W.H.G., Vaughan B., van Paradijs J., 1996, ApJ, 469, L1  
 van Kerkwijk M.H., van Paradijs J., Zuiderwijk E.J., 1995, A&A,

- 303, 497
- Weber F., Glendenning N.K., 1992, *ApJ*, 390, 541
- Weber F., Glendenning N.K., 1993, in Feng D.H., He G.Z., Li X.Q., eds., *Proceedings of the Nankai Summer School, "Astrophysics and Neutrino Physics", Tianjin, China, June 17-27, 1991*, World Scientific, Singapore, pp. 64–183
- Weber F., Weigel M., 1989, *Nucl. Phys. A*, 505, 779
- Weber F., Kettner C., Weigel M.K., Glendenning N.K., 1995, in Vassiliadis G., Panagiotou A., Kumar S., Madsen J., eds., *Proceedings of the International Symposium on Strangeness and Quark Matter*, World Scientific, pp. 308
- Weber F., Schaab C., Weigel M.K., Glendenning N.K., 1997a, in Giovannelli F., Mannocci G., eds., *Vulcano Workshop 1996 Frontier Objects in Astrophysics and Particle Physics, May 27 – June 1, Vulcano*, Italian Physical Society, Bologna (Italia), p. 87
- Weber F., Schaab C., Weigel M.K., Glendenning N.K., 1997b, in Stöcker H., Gallmann A., Hamilton J.H., eds., *Proceedings of the International Conference on Nuclear Physics at the Turn of the Millennium: Structure of Vacuum and Elementary Matter, March 10-16, 1996, Wilderness, South Africa*, World Scientific, Singapore, p. 322
- Wijnands R.A.D., van der Klis M., 1997, *ApJ*, 482, L65
- Wijnands R.A.D., Homan J., van der Klis M., Méndez M., Kuulkers E., van Paradijs J., Lewin W.H.G., Lamb F.K., Psaltis D., Vaughan B., 1997, *ApJ*, 490, L157
- Wijnands R.A.D., Homan J., van der Klis M., Kuulkers E., van Paradijs J., Lewin W.H.G., Lamb F.K., Psaltis D., Vaughan B., 1998a, *ApJ*, 493, L87
- Wijnands R.A.D., Méndez M., van der Klis M., Psaltis D., Kuulkers E., Lamb F.K., 1998b, *ApJ*, 504, L35
- Wijnands R.A.D., van der Klis M., Méndez M., van Paradijs J., Lewin W.H.G., Lamb F.K., Vaughan B., Kuulkers E., 1998c, *ApJ*, 495, L39
- Wiringa R., Fiks V., Fabrocini A., 1988, *Phys. Rev. C*, 38, 1010
- Witten E., 1984, *Phys. Rev. D*, 30, 272
- Yu W., Zhang S.N., Harmon B.A., Paciesas W.S., Robinson C.R., Grindlay J.E., Bloser P., Barret D., Ford E.C., Tavani M., Kaaret P., 1997a, in Dermer C.D., Strickman M.S., Kurfess J.D., eds., *Proceedings of the Fourth Compton Symposium*, AIP Conference Proceedings 410, p. 734
- Yu W., Zhang S.N., Harmon B.A., Paciesas W.S., Robinson C.R., Grindlay J.E., Bloser P., Barret D., Ford E.C., Tavani M., Kaaret P., 1997b, *ApJ*, 490, L153
- Zhang W., Strohmayer T.E., Swank J.H., 1997, *ApJ*, 482, L167
- Zhang W., Jahoda K., Kelley R.L., Strohmayer T.E., Swank J.H., Zhang S.N., 1998a, *ApJ*, 495, L9
- Zhang W., Smale A.P., Strohmayer T.E., Swank J.H., 1998b, *ApJ*, 500, L171
- Zhang W., Strohmayer T.E., Swank J.H., 1998c, *ApJ*, 500, L167